Available online at www.sciencedirect.com
ScienceDirect
Tetrahedron Letters
Tetrahedron Letters 47 (2006) 7671–7675

Synthesis of salicylate dendritic prodrugs

Shengzhuang Tang, Stephen M. June, Bob A. Howell and Minghui Chai*

Department of Chemistry, Central Michigan University, Mt. Pleasant, MI 48859, USA

Received 11 August 2006; revised 29 August 2006; accepted 29 August 2006

Abstract—A small drug molecule, salicylic acid, has been converted into well-defined dendritic macromolecules. The mono-disperse nature of these materials may be clearly shown by NMR and GPC. A third generation salicylic acid dendrimer contains sixty salicylic acid residues, which make up its core, branches, and periphery. Individual salicylic acid moieties in the dendrimer are connected to one another via hydrolyzable diester linkages.

Considerable effort has been devoted to the field of drug delivery devices to prolong the duration of drug release and to deliver a drug selectively to a targeted location, such as a tumor site.[1] Polymers have played an important role in the development of drug delivery systems for controlled release formulations as well as site-directed delivery, since polymeric materials can be easily formulated as microspheres, films, tablets or implantation devices, for achieving sustained drug release with temporal and spatial distribution control in the body.[2] Although many polymers and polymer conjugates have showed promising results as drug carriers during in vitro studies, a large number of them failed when subjected to in vivo examinations, largely as a consequence of polymer-related toxicity or lack of improved therapeutic index.[3] Another crucial limiting factor in the design of polymer-drug conjugates may be low drug carrying capacity.

In the past decade, more attention has been paid to dendrimers as drug-delivery systems because of their cascade three-dimensional structure with nearly perfect monodispersity.[4] Such highly branched architecture along with outer functional termini and inner dendritic nano-voids makes these novel macromolecules more efficient drug carriers when compared with classic polymers. First, the internal cavity of a dendrimer provides an ideal site for a hydrophobic drug to achieve noncovalent encapsulation with the possibility of subsequent controlled release as well as the enhancement of the drug solubility in water. Second, the controllable multivalency of a dendrimer can be used to attach a combination of drug molecules, targeting groups, and solubilizing groups, to the periphery of the dendrimers in a well-defined manner. Third, the more globular shape of dendrimers, instead of the random coil structure of most linear polymers, may enhance their biological performance; furthermore, the low polydispersity of dendrimers should promote reproducible pharmacokinetic behavior.[2] However, the biocompatibility and non-toxicity of dendrimers must be considered before the application for drug delivery; in addition, the formation of dendritic defects (i.e., lack of perfect growth of all arms in a dendrimer) which can result in low drug loading also needs to be carefully controlled during the dendrimer synthesis. Herein is reported the first synthesis of a highly loaded novel dendritic prodrug based on salicylic acid, a commonly used nonsteroidal anti-inflammatory drug (NSAID) (see Fig. 1).

The most attractive feature of the dendritic prodrug is that the drug entities are chemically incorporated into a dendrimer structure, not just attached as pendants on the surface nor physically encapsulated inside the cavities. This design not only incorporates a large number of drug units into the dendritic architecture but also provides the unique potential that the drug molecules can be controllably released via hydrolytic cleavage of ester bonds sequentially and even quantitatively layer by layer from the cascade architecture. In addition, the functional groups at the surface of the novel dendritic drug may be modified to permit the introduction of a synergistic drug. Alternatively, the inner dendritic cavities may be utilized for encapsulation of such a drug. The incorporation of salicylic acid into polymeric

* Corresponding author. Tel.: +1 989 774 3955; fax: +1 989 774 3883; e-mail: chai1m@cmich.edu

0040-4039/$ - see front matter © 2006 Elsevier Ltd. All rights reserved.
doi:10.1016/j.tetlet.2006.08.110

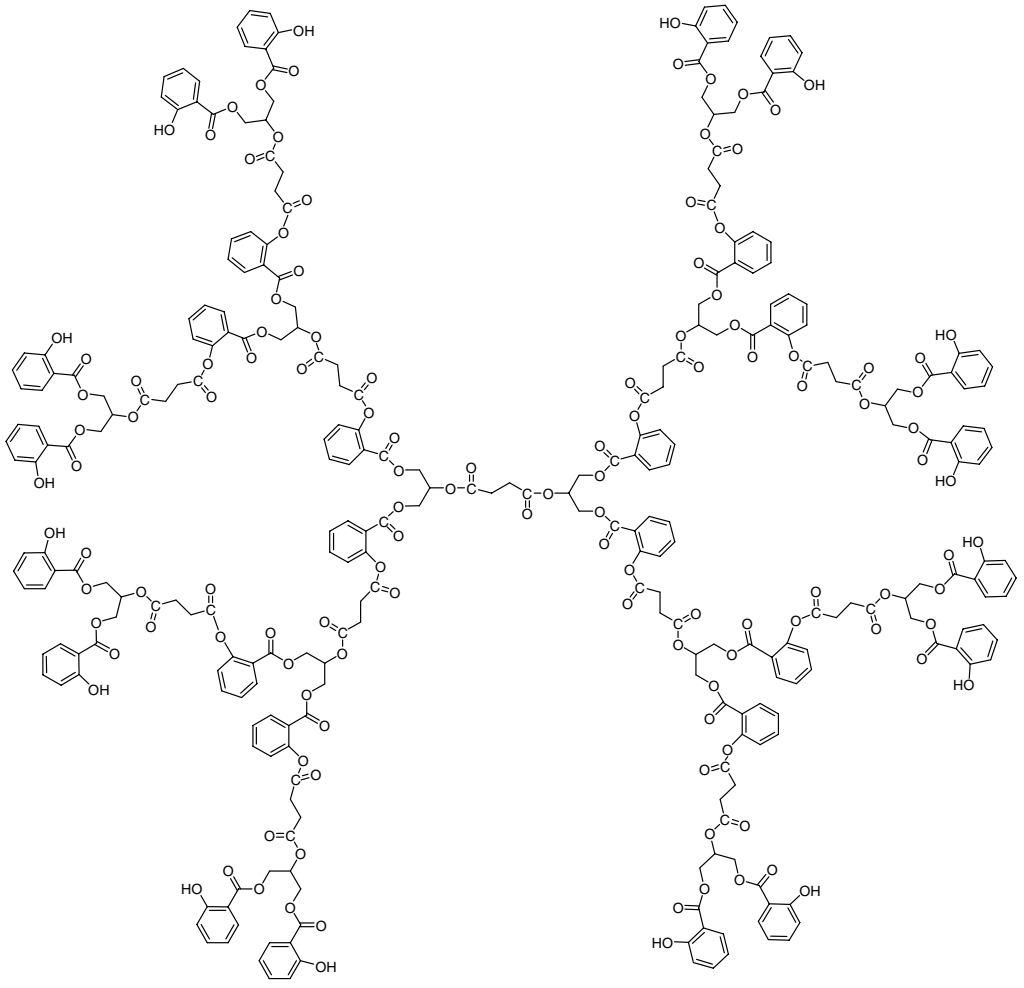

Figure 1. Structure of a dendritic salicylic acid prodrug.

backbones has been reported.[5] Salicylic acid-based polyesters have been shown to display in vitro degradation lag time of a couple of days.[6] The newly synthesized salicylic acid-based dendrimers described here will also be useful for sustained delivery.

Salicylic acid-based dendrimers HO-G*n* ($n = 0$–3: the generation number of the dendrimer) were synthesized by means of 'Lego' or 'click' chemistry[7] using biocompatible building blocks (salicylic acid, glycerol, and succinic acid) by typical stepwise and iterative processes of

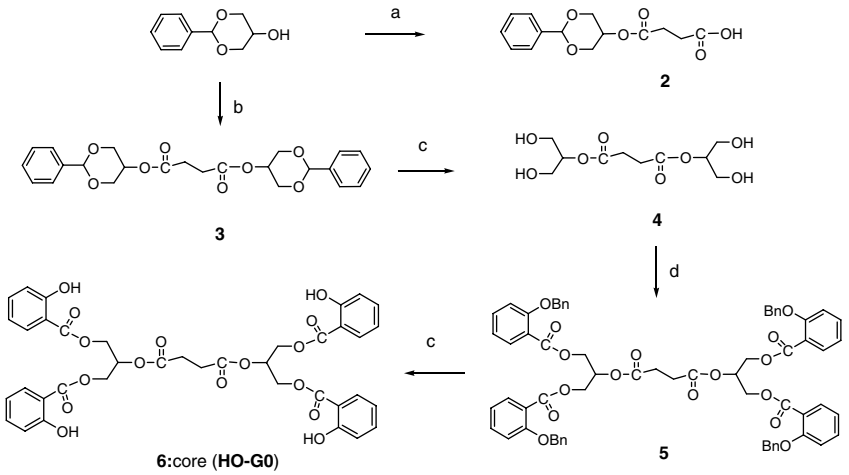

Scheme 1. The syntheses of building block **4** and core **6**. Reagents and conditions: (a) succinic anhydride, pyridine, rt, 18 h, 91%; (b) succinic acid, DCC, DPTS, CH_2Cl_2, rt, 18 h, 87%; (c) 20% $Pd(OH)_2$, 50 psi H_2, THF, rt, 3 h, 85% for **4**, and 94% for **6**; (d) 2-benzyloxybenzoic acid, DCC, DPTS, CH_2Cl_2, rt, 18 h, 78%.

esterification and hydrogenolysis. The glycerol–succinic acid monoester **2** and the pre-core **4** with a tetrahydroxy focal point were first prepared.[8] Compound **4** was coupled to 4 equiv of 2-benzyloxybenzoic acid, followed by subsequent hydrogenolysis to produce the core HO-G0 **6** in an overall 71% yield (Scheme 1).

Compound **2** (4 equiv) was coupled to the core HO-G0, **6**, to afford compound **7**, Ben-G0.5. The benzylidene acetal protecting groups were later removed by hydrogenolysis to provide compound **8**, HO-G0.5, to which the eight units of 2-benzyloxybenzoic acid were then coupled by esterification to yield compound **9**, BnO-G1.0. Again, hydrogenolysis afforded the first generation dendritic drug HO-G1.0, **10**, in an overall 47% yield. The second generation dendritic prodrug **14**, HO-G2.0, was synthesized in four similar steps. Compound **10** was treated with **2** to generate compound **11**. Hydrogenolysis of **11** afforded compound **12**, which were subsequently coupled with 16 units of 2-benzyloxybenzoic acid to produce **13**. The acetal protecting groups were subsequently removed by hydrogenolysis. The third generation dendritic prodrug HO-G3.0, **18**, was prepared in an analogous stepwise procedure, whereby **2** was coupled to **14** followed by hydrogenolysis to afford compound **16**. 2-Benzyloxybenzoic acid was subsequently coupled to **16** followed by routine hydrogenolysis (Scheme 2).

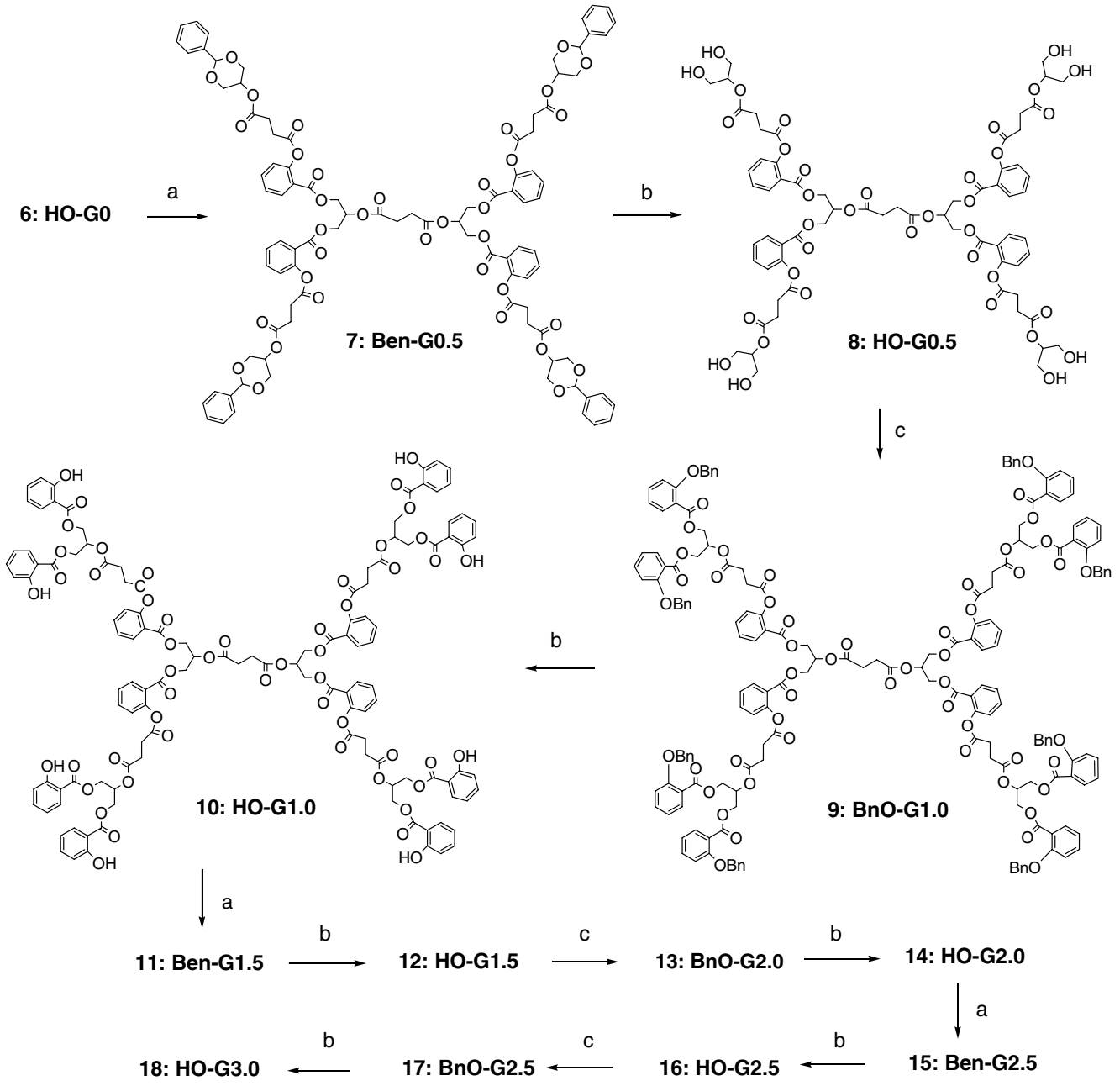

Scheme 2. The syntheses of salicylate dendritic prodrug G1.0–G3.0 (**10**–**18**). Reagents and conditions: (a) Compound **2**, DCC, DPTS, DCM, rt, 18 h for **7**, 24 h for **11**, 36 h for **15**; (b) 20% $Pd(OH)_2$, 50 psi H_2, THF, rt, 3 h; (c) 2-benzyloxybenzoic acid, DCC, DPTS, DCM, rt, 24 h for **9**, 36 h for **13**, 48 h for **17**.

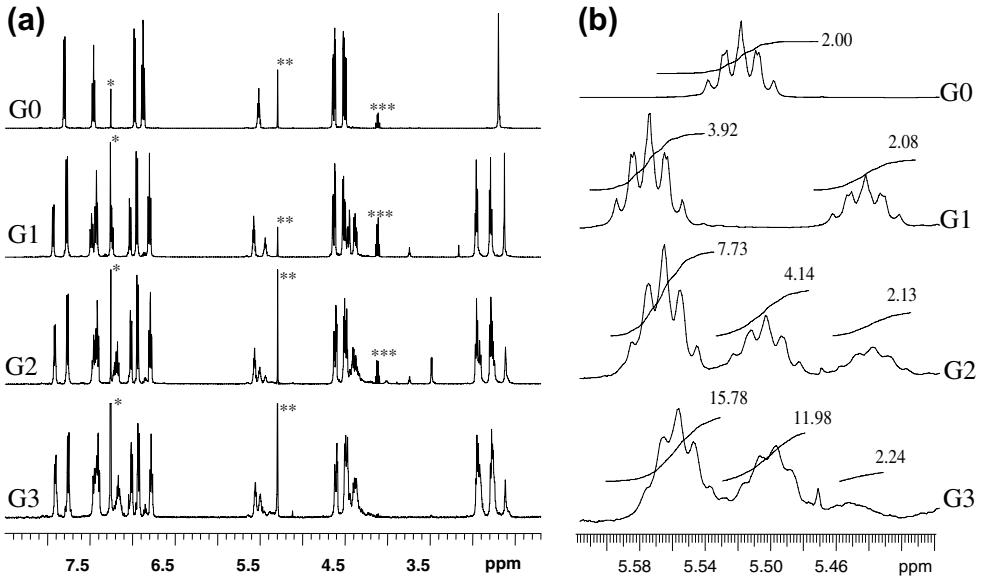

Figure 2. (a) ^{1}H NMR spectra of salicylate dendritic prodrugs G0.0–G3.0, here, *peaks are from the residual protons of the solvent ($CDCl_3$), **peaks are from the protons of CH_2Cl_2 (DCM used as the solvent in the synthesis), and ***peaks are from the methylene protons of ethyl acetate used in the column chromatography separation; (b) the plots of ^{1}H NMR spectral expansions for the methine proton resonance region of the glycerol entities in the salicylate dendritic prodrugs G0.0–G3.0.

The structures of all generations of salicylic acid-based dendrimers were confirmed by FTIR, ^{1}H and ^{13}C NMR, and MALDI-TOF-MS.[8] The strong O–H characteristic stretch around 3220 cm^{-1} in the FTIR spectrum confirmed the presence of free hydroxyls in the dendritic structures. The ^{1}H NMR spectra (Fig. 2) of the different generation dendritic drug HO-G*n* ($n = 0$–3) exhibit a clear correlation of the growth of higher generation dendrimers with the increasing characteristic sets of well resolved peaks. Additionally, the relative integration area of exterior and interior benzyl and glycerol proton resonances in the NMR spectra clearly indicates that the next higher generation of the desired prodrugs had been formed from the previous generation, that is, the conversion of one generation to the next was cleanly accomplished.[9]

The polydispersity indices (PDI) of these dendritic prodrugs listed in Table 1 were determined by gel-permeation chromatography (GPC) (Fig. 3), indicating the high purity and monodispersity of the dendrimers formed.[10]

This represents the first synthesis of salicylic acid-based dendrimers. These newly synthesized dendritic prodrugs

Table 1. GPC data for the dendritic salicylate prodrugs G0.0–G3.0

Dendrimer	Retention volume (mL)			PDI (Mw/Mn)		
	Run 1	Run 2	Average	Run 1	Run 2	Average
G0.0	10.22	10.21	10.22	1.030	1.031	1.031
G1.0	9.59	9.59	9.59	1.042	1.040	1.041
G2.0	9.15	9.15	9.15	1.056	1.049	1.053
G3.0	8.83	8.82	8.83	1.044	1.047	1.046

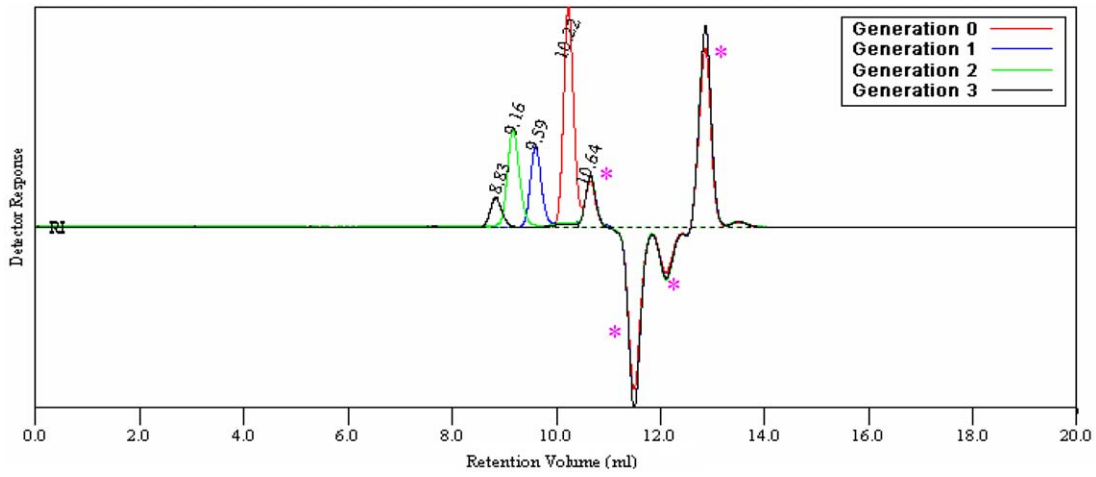

Figure 3. Overlay of GPC chromatograms of salicylate dendritic prodrugs G0.0–G3.0. Here, *peaks are from the solvent (THF).

possess a number of drug entities cascading from the core, interior and exterior regions, and also display a large number of functional groups at the periphery. Such a novel dendritic prodrug design provides a promising hydrolyzable drug delivery system for sequential and quantitative drug release. With a much higher drug loading than has heretofore been archived, the dendritic prodrug could potentially greatly exceed the effectiveness of the current repertoire of drug vehicles and offer a new platform for drug delivery.

Acknowledgements

Support for this research from US National Science Foundation (NUE-0407298), Research Corporation (CC-6059), American Chemical Society Petroleum Research Fund (PRF # 40998-GB4) and Central Michigan University (FRCE and PRIF) is gratefully acknowledged.

References and notes

1. Degroot, F. M.; Damen, E. W.; Scheeren, H. W. *Curr. Med. Chem.* **2001**, *8*, 1093.
2. Li, Y.-Q.; You, H.-B. *Pharm. Res.* **2006**, *23*, 1.
3. Duncan, R. *Anti-Cancer Drugs* **1992**, *3*, 175.
4. Svenson, S.; Tomalia, D. A. *Adv. Drug Delivery Rev.* **2005**, *57*, 2106.
5. Kricheldorf, H.; Gerken, A.; Yulchibaev, B.; Friedrich, C. *J. Polym. Sci., Part A: Polym. Chem.* **2000**, *38*, 2013.
6. Schmeltzer, R.; Schmealenberg, K.; Uhrich, K. *Biomacromolecules* **2005**, *6*, 359.
7. (a) Maraval, V.; Caminade, A.-W.; Majoral, J.-P.; Blais, J.-C. *Angew. Chem., Int. Ed.* **2003**, *42*, 1822–1826; (b) Maraval, V.; Pyzowski, J.; Caminade, A.-W.; Majoral, J.-P. *J. Org. Chem.* **2003**, *68*, 6043–6046; (c) Wu, P.; Feldman, A. K.; Nugent, A. K.; Hawker, C. J.; Scheel, A.; Voit, B.; Pyun, J.; Fréchet, J. M. J.; Sharpless, K. B.; Fokin, V. V. *Angew. Chem., Int. Ed.* **2004**, *23*, 3928–3932.
8. Luman, N.; Smeds, K.; Grinstaff, M. *Chem. Eur. J.* **2003**, *9*, 5618.
9. *Spectroscopic data of the dendritic salicylate prodrugs G0.0–G3.0*: HO-G0 **6**: ^{1}H NMR ($CDCl_3$) (500 MHz, ppm): 2.699 (4H, s, succ.-CH_2), 4.490–4.526 (4H, m, Glycerol–CH_2), 4.617–4.651 (4H, m, Glycerol–CH_2), 5.521 (2H, pentet, $J = 5.0$ Hz, Glycerol–CH), 6.878 (4H, td, $J = 7.5$ and 1.0 Hz, Ar-H), 6.977 (4H, dd, $J = 8.5$ and 1.0 Hz, Ar-H), 7.462 (4H, td, $J = 8.0$ and 1.0 Hz, Ar-H), 7.805 (4H, dd, $J = 8.0$ and 1.5 Hz, Ar-H); ^{13}C NMR ($CDCl_3$) (75 MHz, ppm): 28.838 (succ.-CH_2), 62.747 (Glycerol–CH), 69.095 (Glycerol–CH_2), 111.687, 117.700, 119.363, 129.893, 136.203, and 161.742 (Ar-C), 169.471 (Ar-CO), 171.249 (succ.-CO); MALDI-TOF-MS observed: $[M+Na]^+$ 769.0 and $[M+K]^+$ 785.0; calculated for $C_{38}H_{34}O_{16}$: 746.2.
HO-G1 **10**: ^{1}H NMR ($CDCl_3$) (500 MHz, ppm): 2.631(4H, s, core succ.-CH_2), 2.792 (8H, t, $J = 6.8$ Hz, exterior succ.-CH_2), 2.961 (8H, t, $J = 6.8$ Hz, exterior succ.-CH_2), 4.362–4.398 (4H, m, core Glycerol–CH_2) 4.446–4.479 (4H, m, core Glycerol–CH_2), 4.497–4.532 (8H, m, exterior Glycerol–CH_2), 4.616–4.649 (8H, m, exterior Glycerol–CH_2), 5.445 (2H, t, $J = 5.0$ Hz, core Glycerol–CH), 5.576 (4H, t, $J = 5.0$ Hz, exterior Glycerol–CH), 6.804 (8H, td, $J = 4.0$ and $J = 1.0$ Hz, exterior Ar-H), 6.950 (8H, d, $J = 7.5$ Hz, exterior Ar-H), 7.121 (4H, dd, $J = 8.0$ and $J = 1.0$ Hz, core Ar-H), 7.248 (4H, td, $J = 7.5$ and $J = 1.0$ Hz, core Ar-H), 7.428 (8H, td, $J = 7.0$ and $J = 1.5$ Hz, exterior Ar-H), 7.486 (8H, td, $J = 7.0$ and 1.5 Hz, exterior Ar-H), 7.774 (8H, dd, $J = 8.0$ and 1.5 Hz, exterior Ar-H), 7.934 (4H, dd, $J = 8.0$ and 1.5 Hz, core Ar-H), 10.485 (8H, s, Ar-OH); ^{13}C NMR ($CDCl_3$) (75 MHz, ppm): 28.731 (core succ.-CH_2), 28.914 and 29.021 (exterior succ.-CH_2), 62.770 and 62.853 (exterior and core Glycerol–CH), 69.011 and 69.225 (exterior and core Glycerol–CH_2), 111.680, 117.647, 119.371, 129.916, 136.58, and 161.696 (exterior Ar-C), 122.133, 123.827, 126.177, 131.702, 134.281, and 150.770 (core Ar-C), 163.444 (Ar-CO), 169.494, 170.746, and 171.364 (succ.-CO); MALDI-TOF-MS observed: $[M+Na]^+$ 2427.4 and $[M+K]^+$ 2443.4; calculated for $C_{122}H_{106}O_{52}$: 2404.1.
HO-G2 **14**: ^{1}H NMR($CDCl_3$) (500 MHz, ppm): 2.620 (4H, s, core succ.-CH_2), 2.749–2.803 (24H, m, exterior and middlesucc.-CH_2), 2.912–2.976 (24H, m, exterior and middle succ.-CH_2), 4.337–4.422 (12H, m, interior Glycerol–CH_2), 4.439–4.516 (28H, m, exterior and interior Glycerol–CH_2), 4.601–4.634 (16H, m, exterior Glycerol–CH_2), 5.446 (2H, m, core Glycerol–CH), 5.509 (4H, p, $J = 5.0$ Hz, middle Glycerol-CH), 5.570 (8, p, $J = 5.0$ Hz, exterior Glycerol–CH), 6.793 (16H, t, $J = 7.5$ Hz, exterior Ar-H), 6.943 (16H, d, $J = 8.0$ Hz, exterior Ar-H), 7.014–7.030 (12H, m, interior Ar-H), 7.403–7.481 (28H, t, exterior and interior Ar-H), 7.766 (16H, dd, $J = 8.0$ and 1.5 Hz, exterior Ar-H), 7.911–7.927 (12H, m, interior Ar-H); ^{13}C NMR ($CDCl_3$) (75 MHz, ppm): 28.922 and 29.036 (succ.-CH_2), 62.869 (Glycerol–CH), 69.026 and 69.324 (Glycerol–CH_2), 111.703, 117.639, 119.371, 129.924, 136.142, and 161.704 (exterior Ar-C), 122.156, 123.797, 123.926, 126.177, 131.709, 134.227, 150.747, and 150.876 (interior Ar-C), 163.360 and 163.482 (Ar-CO), 169.494, 170.723, 170.807, 171.356, and 171.410 (succ.-CO); MALDI-TOF-MS observed: $[M+Na]^+$ 5742.4; calculated for $C_{290}H_{250}O_{124}$: 5719.0.
HO-G3 **18**: ^{1}H NMR ($CDCl_3$) δ ^{1}H (500 MHz, ppm): 2.622 (4H, s, core succ.-CH_2), 2.761–2.796 (56H, m, succ.-CH_2), 2.923–2.966 (56H, m, succ.-CH_2), 4.334–4.405 (28H, m, interior Glycerol–CH_2), 4.446–4.508 (60H, m, exterior and interior Glycerol–CH_2), 4.593–4.625 (32H, m, exterior Glycerol–CH_2), 5.452 (2H, m, core Glycerol–CH), 5.501 (12H, m, middle Glycerol–CH), 5.561 (16H, p, $J = 5.0$ Hz, exterior Glycerol–CH), 6.783 (32H, t, $J = 7.5$ Hz, exterior Ar-H), 6.934 (32H, d, $J = 8.5$ Hz, exterior Ar-H), 7.004–7.021 (28H, m, interior Ar-H), 7.129–7.215 (28H, m, interior Ar-H), 7.393–7.466 (60H, m, exterior and interior Ar-H), 7.758 (32H, d, $J = 8.0$, exterior Ar-H), 7.892–7.918 (28H, m, interior Ar-H), 10.474 (32H, s, Ar-OH); ^{13}C NMR ($CDCl_3$) (75 MHz, ppm): 28.922 and 29.036 (succ.-CH_2), 62.869 (Glycerol–CH), 69.034 and 69.324 (Glycerol–CH_2), 111.710, 117.639, 119.371, 129.931, 136.142, and 161.696 (exterior Ar-C), 122.164, 123.789, 126.185, 131.709, 134.227, 150.739, and 150.854 (interior Ar-C), 163.390 and 163.489 (Ar-CO), 169.494, 170.730, 170.814, 171.356, and 171.417 (succ.-CO); MALDI-TOF-MS observed: $[M+H]^+$ 12349.7; calculated for $C_{290}H_{250}O_{124}$: 12348.5.
10. *GPC experimental*: All samples were analyzed using a Viscotek GPCmax VE 2001 Module equipped with a Viscotek TDA 302 Triple Detector Array, a ViscoGEL microstyrogel mixed-bed column, linear poly(styrene) calibration and THF as elution solvent at 1.0 mL/min.